Type of the Paper (Article)

A Fuzzy Inference System for Unsupervised Deblurring of Motion Blur in Electron Beam Calibration

Salaheddin Hosseinzadeh [1,*]

[1] Brunel University; salaheddin.hosseinzadeh@gmail.com
* Correspondence: salaheddin.hosseinzadeh@gmail.com

Abstract: This paper presents a novel method of restoring the electron beam (EB) measurements that are degraded by linear motion blur. This is based on a Fuzzy Inference System (FIS) and Wiener inverse filter, together providing autonomy, reliability, flexibility and real-time execution. This system is capable of restoring highly degraded signals without requiring the exact knowledge of EB probe size. The FIS is formed of three inputs, eight fuzzy rules and one output. The FIS is responsible to monitor the restoration results, grade their validity and choose the one that yields to a better grade. These grades are produced autonomously by analyzing results of Wiener inverse filter. To benchmark the performance of the system, ground truth signals obtained using an 18 um wire probe are compared with the restorations. Main aims are therefore a) Provide unsupervised deblurring for device independent EB measurement; b) Improve the reliability of the process; c) Apply deblurring without knowing the probe size. These, further facilitate the deployment and manufacturing of EB probes and probe independent and accurate EB characterization. The paper findings also makes restoration of previously collected EB measurements easier, where the probe sizes are not known or recorded.

Keywords: Fuzzy Inference System; Fuzzy Logics; Linear Motion Blur; Fuzzy Deblurring; Electron Beam Calibration; Signal & Image Processing

---

1. Introduction

The main goal of fuzzy systems is to define and control sophisticated processes by incorporating and taking advantage of human knowledge and experience. Nowadays, fuzzy logics are widely used in industry for various applications ranging from cameras, to cement kilns, trains and vacuum cleaners [1]. Furthermore, deblurring techniques have versatile applications and they are either performed in spatial [2] or frequency domains [3-5]. Author in [6] modeled the EB measurement process with a linear motion blur and evaluated three of the well-established deblurring techniques for EB restoration. In this study [6] author used Weiner inverse filter, Blind and Richardson-Lucy deconvolutions to restore the EB distribution and correct the measurements through deblurring. A simple motion blur is formulated in equation. 1.

$$g(x) = \int f(x)h(x) + n(x) \tag{1}$$

Where in the spatial domain f, g, h and n are the ground-truth signal (EB distribution) of length L_f, degraded signal (measurement from probe), point spread function (PSF) of length L_h and noise respectively, with their frequency domains being represented by uppercase letters F, G and H. In case of electron beam measurements, the ground through signal is the distribution of EB, and the degraded signal is the measurement acquired from the probe. The electron absorption of a slit or wire probe of size L_h is modeled with a PSF kernel [6].

Linear motion blur point spread function has two distinct characteristics of motion direction and length (L) [7]. The PSF is known for having harmonically spaced vanishing magnitudes in the frequency domain due to its limited length in the spatial domain [8]. There are several approaches to estimate L_h such as log power spectrum, cepstrum, bispectrum, and pitch detection algorithms. In image deblurring jargon, it is assumed that the frequency spectrum of F is smooth and does not contain vanishing frequencies, hence any vanishing frequencies in G are associated to H [9][10]. However, this assumption usually does not hold for EB measurements, especially where the L_f is in the same order of L_h. This similarity makes it complicated to distinguish between L_f and L_h and therefore compromises the deblurring process by an incorrect detection of null frequencies. Such erroneous deblurring process is likely to produce an incorrect but convincing result, notably when f and h have remarkable cross-correlation. This ambiguity is likely to happen in EB measurements, because a) f and h are usually in the same order of magnitude and they have relatively high cross-correlation; b) the L_f can be inconsistent. In [6], a prior knowledge of L_h is used to estimate the position of null frequency of h from the spectrum analysis of G. The author limited the spectrum of G to ±15% of the nominal L_h by applying a window to its log-power spectrum, therefore, ignoring vanishing frequencies outside of this interval, this algorithm is available in [11]. This strategy relies on knowing the L_h therefore, it is a good approach when it is known accurately. There are few limitations with this method due to the varying nature of L_f during the calibration and even measurement process. As a result, the beam's vanishing frequency (or its harmonics) could be located within the applied window and cause a false detection. Furthermore, if the inaccuracy of L_h is more than 15% the null frequency of h is ignored by the window, resulting in an erroneous restoration. In addition, any inaccuracy more than ±15% cannot be compensated.

One solution to effectively address this uncertainty is to use fuzzy systems. Fuzzy inference systems are widely used to address instrumental uncertainties, a comprehensive review and explanation of fuzzy inference systems are provided in [12].

It is known that a wrong estimation of L_h can lead to drastic noise-like errors in the restorations [13]. Furthermore, utilizing deblurring techniques for industrial purposes requires real-time, reliable and unsupervised methods. To satisfy these requirements, this article proposed a Wiener filter that is monitored by a Fuzzy Inference System. Wiener filter is selected due to its simplicity, real-time execution and superior performance in the restoration of linear motion blur [6]. The fuzzy inference system deals with the uncertainty of the deconvolution process, it controls the whole restoration process and it comprised of three crisp inputs that includes the PSF length or probe size (L_h) deviation, attenuation of the vanishing frequencies and deconvolution residue.

However, probe size deviation is an optional input, which is based on a previous rough knowledge of L_h. If L_h is roughly known, it serves as a reference point from which the PSF length deviation is calculated. Therefore, unlike [6], prior knowledge of L_h does not limit the inaccuracy compensation to ±15%. It is demonstrated in [6] that the spatial domain of h, has a sharper transition compared to the EB distribution (f). This is due to the semi-Gaussian distribution of f compared to h. Therefore, vanishing frequencies of h are expected to have higher attenuation or lower magnitude compared to f. Hence, the normalized magnitude of the detected null frequencies in G are the second crisp input to the FIS. The last input of the system is the quantified deblurring artifacts that are introduced during the restoration of f from g. The restored beam distributions are denoted as ($\hat{f}$). These residual artifacts are inevitable and they increase as the h deviates from its mathematical definition. Extraction of residues from $\hat{f}$ is explained in section II. The output of the fuzzy system (E_i) is defuzzified to represent the quality of the restorations. This output is generated based on the definition of the fuzzy rules that are explained in the next section.

The rest of this paper is arranged as follows. Section II, illustrates the details of FIS implementation. This includes specifying the crisp inputs and fuzzifying them, defining the membership functions and formulating the fuzzy sets. The section continues by identifying the fuzzy rules and making an inference to generate the output. Section III, presents the practical results of

Preprints (www.preprints.org) | NOT PEER-REVIEWED | Posted: 19 October 2018 doi:10.20944/preprints201810.0432.v1

Peer-reviewed version available at *Appl. Syst. Innov.* **2018**, *1*, 48; doi:10.3390/asi1040048

proposed method and the ability of the system to distinguish the correct deblurring results. The values of membership functions parameters are provided and a comparison is made between implementing the fuzzy system with and without the knowledge of probe size (L_h).

2. Modeling and Implementation

As mentioned, when there is similarity between L_f and L_h it is difficult to discriminate between their null frequencies just by looking at G. This introduces an uncertainty and makes it hard to decide which null frequency belongs to the probe (H), because null frequencies can belong to either beam (F) or probe (H). To address the uncertainty of unsupervised L_h detection, all the null frequencies in G are identified and only the first two nulls with lowest frequencies are extracted, while avoiding the harmonics. This implies that maximum of two null frequencies ($\omega_{i=\ 1,2}$) are to be extracted from G. There are three possibilities based on the extracted number of null frequencies: a) If no null frequency is detected due to $L_h \ll L_f$, then motion blur effect is negligible and deconvolution is not necessary; b) If a single null frequency is detected, as a result of $L_h \gg L_f$, then the deconvolution can progress without involving the fuzzy system as the null frequency belongs to L_h; c) In case two null freqsuencies are extracted (ω_1, ω_2), two deconvolutions are performed, where each of the deconvolutions are performed by adjusting their corresponding $\hat{L}_{i=1,2}$ ($\hat{L}_{i=1,2} \propto 1/\omega_{i=1,2}$). This is done because both ω_1 and ω_2 could be belonging to h of different sizes.

A FIS is defined with three merits to grade the deblurrings. Deblurrings are performed by two individual Weiner filter that uses $\hat{L}_1$ and $\hat{L}_2$ resulting in $\hat{f}_1$ and $\hat{f}_2$ respectively. The fuzzy system produces a single crisp output, *deconvolution grade* ($E_{i=1,2}$) for each restoration. The restoration process that produces a higher E_i is then chosen as the correct process with its corresponding $\hat{L}_i$ being the correct probe size ($L_h \leftarrow \hat{L}_i$). A single layer (non-hierarchal) fuzzy inference system of three inputs and a single output is designed to evaluate the overall deblurring process. These inputs are: PSF length deviation, null frequency magnitude and residues, and the deconvolution grade is the only output. These inputs and the output are explained in details as follows.

2.1. PSF length deviation

As mentioned, ω_1 and ω_2 are extracted to accurately adjust the L_h during the restoration process. By having rough prior knowledge of the probe size (L_h) and the estimated sizes ($\hat{L}_i$) from G, we can define PSF length deviation as the distance between expected and the estimations ($|L_h - \hat{L}_i|$). This definition converges to zero if the estimation is close to the prior knowledge, whereas, it increases if $\hat{L}_i$ is deviated from L_h. Two fuzzy sets (A_{far} & A_{close}) with membership functions of μ'_m and μ_m are defined to account for the probe inaccuracy and assign a degree of membership to each $\hat{L}_i$ based on its deviation from L_h. Membership functions are defined by polynomial-Z (zmf) and polynomial-S (smf). The A_{close} fuzzy set definition and its membership function is formulated in equation 2. A thorough evaluation of fuzzy membership functions are provided in [14].

$$A_{close} = \{(\hat{L}_i, \mu_{m(\hat{L}_i)})|\ \ 0 < \hat{L}_i < \infty\ \ , m(\hat{L}_i) = \frac{2|L_h - \hat{L}_i|}{L_h}\}$$

$$\mu_m = \begin{cases} 1 & m \le a_m \\ 1 - 2\left(\dfrac{m - a_m}{c_m - a_m}\right)^2 & a_m < m \le \dfrac{a_m + c_m}{2} \\ 2\left(\dfrac{m - c_m}{c_m - a_m}\right)^2 & \dfrac{a_m + c_m}{2} < m \le c_m \\ 0 & m > c_m \end{cases} \tag{2}$$

Where a_m and c_m are the membership function parameters that are found heuristically through analysis of several measurements.

2.2. Null frequency magnitude

Preprints (www.preprints.org) | NOT PEER-REVIEWED | Posted: 19 October 2018 doi:10.20944/preprints201810.0432.v1

Peer-reviewed version available at *Appl. Syst. Innov.* **2018**, *1*, 48; doi:10.3390/asi1040048

The second input of the fuzzy system is the magnitude of the extracted null frequencies. This is extracted from the normalized log-power spectrum of g, and has a dynamic range of 0 to 1 dB, demonstrated in Figure 1.

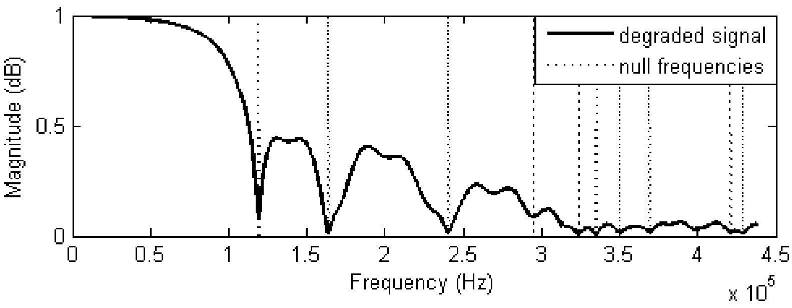

Figure 1. Normalized power spectrum of G exhibits ω_1 and ω_2 at 0.12 and 0.165 MHz frequencies, with their harmonics at higher frequencies.

As explained, h is most likely to have rapid spatial transitions compared to f, this implies that H is likely to have the nulls with higher attenuation in G (nulls with lower magnitude). As a result, two fuzzy sets (B_{high} & B_{Low}) with membership functions of μ'_o and μ_o are defined to assign a higher membership value to the nulls with more attenuation (or lower magnitude); whereas, a lower degree of membership is assigned to less attenuated (higher magnitude) nulls. Membership functions are defined with zmf and sfm. B_{Low} is formulated in equation 3, where G_N is the normalized frequency spectrum of the degraded signal g and a_o and c_o are the membership function parameters. A_{Far} membership function definition is similar to B_{Low} as they are both defined by smf.

$$B_{Low} = \{(\hat{L}_i, \mu'_{o(\omega_i)}) | 0 < \hat{L}_i < \infty, o(\omega_i) = \log(|G_N(\hat{L}_i) + 1|)\}$$

$$\mu'_o = \begin{cases} 0 & o \leq a_o \\ 2\left(\dfrac{o - a_o}{c_o - a_o}\right)^2 & a_o < o \leq \dfrac{a_o + c_o}{2} \\ 1 - 2\left(\dfrac{o - c_o}{c_o - a_o}\right)^2 & \dfrac{a_o + c_o}{2} < o \leq c_o \\ 1 & o > c_o \end{cases} \tag{3}$$

2.3. Deconvolution artifact residues

Deconvolutions are performed using the Wiener inverse filtering process in equation 4.

$$\hat{F}_i = \frac{1}{H(\omega_i)} \left[\frac{|H(\omega_i)|^2}{|H(\omega_i)|^2 + \dfrac{1}{SNR(\omega)}} \right] G(\omega) \tag{4}$$

Where in the frequency domain, $\hat{F}_i$ is the restored ground truth signal and SNR is the signal to noise ratio. After the deconvolutions, $\hat{f}_{i=1,2}$ has shorter lengths in spatial domain, compared to g. We first normalized g and both of the restorations ($\hat{f}_{i=1,2}$) between $[0, -1]$, g_N is then shifted so its minimum is matched with the minimums of each $\hat{f}_i$ in the spatial domain to obtain $\hat{g}_N$. Finally, every restoration residue (r_i) is quantified as in equation 5.

$$r_i = \frac{4}{\int g(x)\ dx} \cdot \int \hat{f}_i(\tau)\ d\tau \qquad \{\tau \in x | \hat{g}_N(\tau) > \ -0.05\} \tag{5}$$

Preprints (www.preprints.org) | NOT PEER-REVIEWED | Posted: 19 October 2018 doi:10.20944/preprints201810.0432.v1

Peer-reviewed version available at Appl. Syst. Innov. 2018, 1, 48; doi:10.3390/asi1040048

The deconvolution process using both of the extracted PSFs and their corresponding residues are showed in Figure 2. The deconvolution was performed with a Wiener inverse filter, where h is formulated in equation 6.

$$h_{\hat{L}_i}(x) = \begin{cases} 0 & o.w \\ 1 & |x| < \dfrac{\hat{L}_i}{2} \end{cases} \tag{6}$$

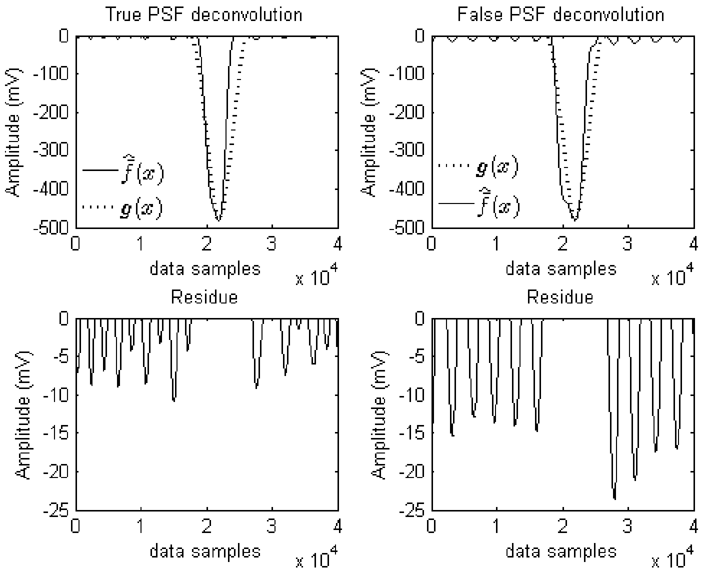

Figure 2. Deconvolution of the degraded pulse in Figure 1, using two different PSF lengths and demonstration of their deconvolution residues.

Two fuzzy sets (C_{low} and C_{high}) are defined with membership functions of μ_r and μ_r' using zmf and smf respectively, where the overall shape of the functions are determined by a_r and c_r. These functions are designed to assign a higher degree of membership to the $\hat{L}_i$ that produces a smaller amount of residues after restoration.

2.4. Deconvolution grade

All the combinations of the aforementioned inputs are used to form 8 if-then rule statements with different weights. These statements with their corresponding weights are provided in Table 1. Fuzzy AND operator is then used for the implication of the fuzzy consequences.

Table. 1. Rule base formation criteria.

Antecedent			**Consequence**	**Rules Weight**
PSF Dev	Attenuation	Residue	Restoration quality	
μ_m	μ_o	μ_r	μ_g	1
μ_m	μ_o	μ_r'	μ_g	0.66
μ_m	μ_o'	μ_r	μ_g	0.66
μ_m	μ_o'	μ_r'	μ_b	0.66
μ_m'	μ_o	μ_r	μ_g	0.66
μ_m'	μ_o	μ_r'	μ_b	0.66
μ_m'	μ_o'	μ_r	μ_b	0.66
μ_m'	μ_o'	μ_r'	μ_b	1

Peer-reviewed version available at Appl. Syst. Innov. 2018, 1, 48; doi:10.3390/asi1040048

Rule weight is added to scale the consequences and account for the certainty of the rules. The consequence is the restoration quality with two fuzzy sets (D_{good} & D_{bad}) and membership functions of μ_q and μ'_q respectively defined by smf and zmf. Aggregations of the rules are performed by using Zadeh T-Norm, and defuzzifications are carried out by mean of maximum (MoM) method [15]. The resulting crisp values are the *deconvolution grades* ($E_{i=1,2}$), therefore; there is a grade ($E_{i=1,2}$) for each deconvolution. In other words, for each $\hat{f}_{i=1,2}$ that is deblured by its corresponding $h_{\hat{L}_{i=1,2}}$ there is an overall grade of restoration ($E_{i=1,2}$). According to the definition of the consequence membership functions, a greater value of E_i represents a better restoration and in contrary a lower value of E_i represents a possible erroneous process, (E_i is ranging from 0 to 1). With this proposed system, if by mistake L_f is used instead of L_h in the formation of the h (equation 6) then the resulting E_i will be lower. Overall, E_1 and E_2 are used comparatively to determine and select the best restoration between $\hat{f}_1$ and $\hat{f}_2$ that are emerged from restoring a degraded sample (g). This proposed system and its overall restoration processes are demonstrated in Figure 3.

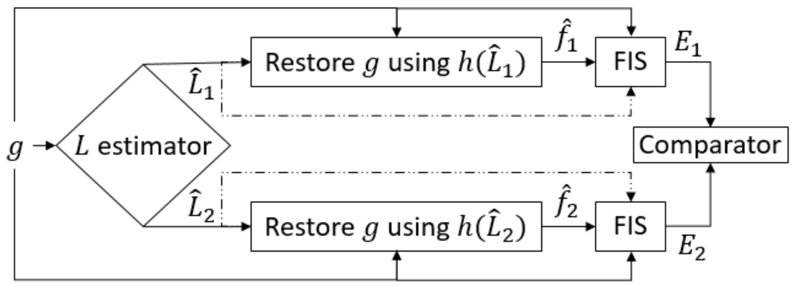

Figure 3. Process diagram, $\hat{L}_i$ connections to FIS are optional.

3. Practical Result

3.1. Membership function parameters

Membership function parameters are investigated pragmatically by testing the explained algorithm for various degraded EB measurement samples. In all degraded measurements, h and f had approximately similar sizes as a result of which $\hat{L}_1 \cong \hat{L}_2$. The membership functions are designed with smooth transitions, to provide a general solution and more flexibility, except for the attenuation. To further discriminate between E_1 and E_2 the attenuation membership functions parameters were adjusted to have more emphasize between the interval of 0 to 0.3dB. This intuitive definition is done by observing the magnitude of null frequencies in several degraded signals, where the attenuation of the null frequencies were always under 0.3dB. The membership functions parameters are presented in Table 2.

Table 2. Membership function definition details.

PSF Deviation				Attenuation				Residue				Restoration Quality			
μ_m		μ'_m		μ_o		μ'_o		μ_r		μ'_r		μ_q		μ'_q	
a_m	c_m	a_m	c_m	a_o	c_o	a_o	c_o	a_r	c_r	a_r	c_r	a_q	c_q	a_q	c_q
0.02	1	0.04	1	0.02	0.3	0.05	0.3	0	1	0	1	0	1	0	1

The membership functions of attenuation (B_{high} & B_{Low}) and residue (C_{low} & C_{high}) fuzzy sets, are depicted in Figure 4, according to their values in Table 2. The fuzzy sets of PSF deviation and restoration quality are also defined with the similar membership functions to that of residues.

Preprints (www.preprints.org) | NOT PEER-REVIEWED | Posted: 19 October 2018 doi:10.20944/preprints201810.0432.v1

Peer-reviewed version available at Appl. Syst. Innov. 2018, 1, 48; doi:10.3390/asi1040048

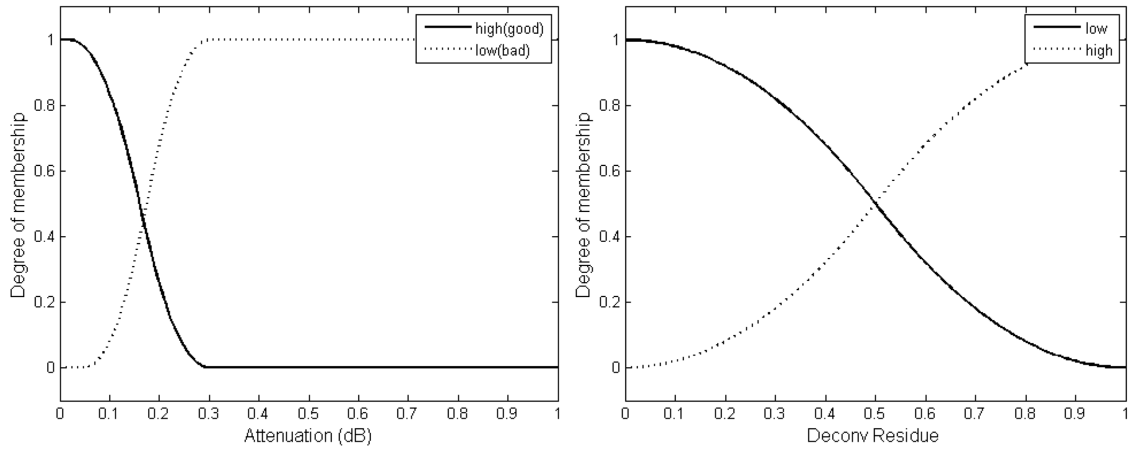

Figure 4. Attenuation, and Deconvolution Residue membership functions.

The analysis of few of the samples are showed in Figure 5 and 6. For few of EB measurements the L_h (probe sizes) were known to be 1.00, 0.20 and 0.40 mm respectively. The crisp fuzzy inputs and deconvolution grades E_i are also provided for every sample. The restoration that resulted in the higher E_i is selected by the system as the correct solution and its corresponding $\hat{L}_i$ therefore, represents the probe size ($\hat{L}_h \leftarrow \hat{L}_i$). To validate the proposed system, with the ground truth signal (f) [6], both restorations ($\hat{f}_{1,2}$) were compared against their ground truth signal using cross-correlation. For all the $\hat{f}_i$ with the higher E_i, the cross-correlation of $\hat{f}_i$ and f also produced greater coefficients, supporting the accuracy and reliability of the system. As another benchmark, full width at half maximum (FWHM) analysis is used, as it is a popular measure in the EB calibration jargon. The FWHM of f and the $\hat{f}_i$ that has the higher E_i produced similar result, further confirming that the FIS has successfully identified the correct restoration process.

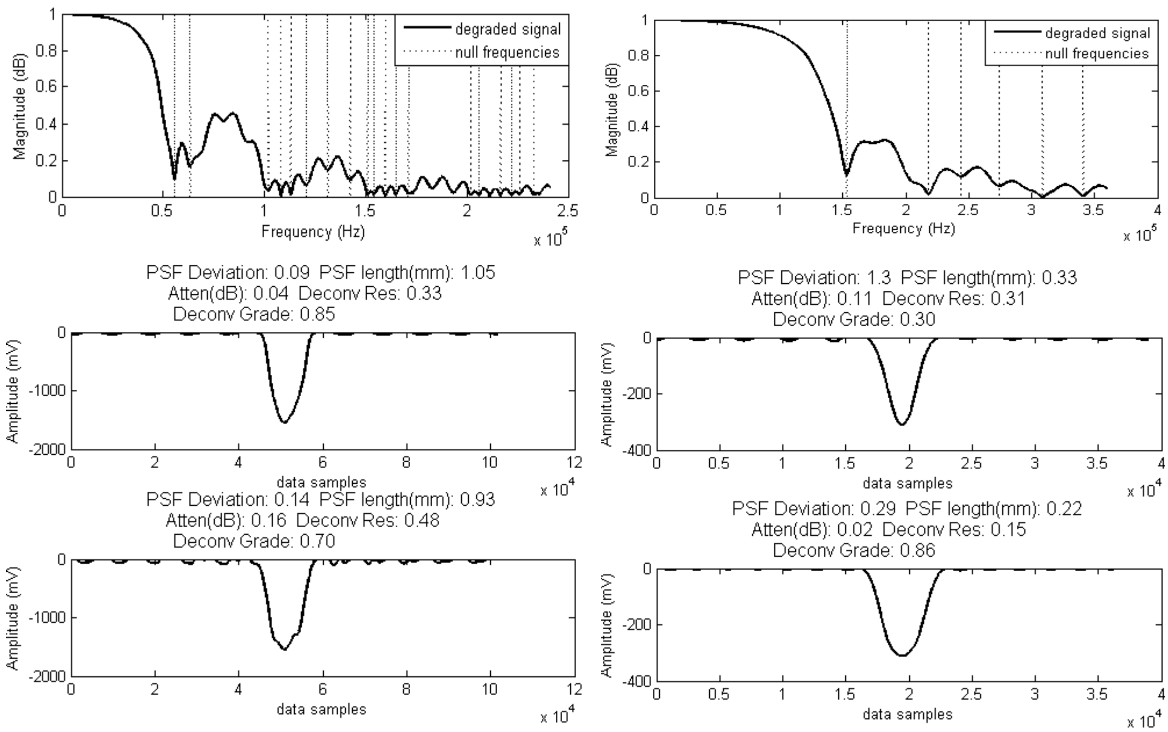

Figure 5. Null frequencies in the spectrum of the degraded pulse. Result of restoration with detected null frequencies, expected PSF length of 1mm on the left, and 0.2mm on the right.

Peer-reviewed version available at *Appl. Syst. Innov.* **2018**, *1*, 48; doi:10.3390/asi1040048

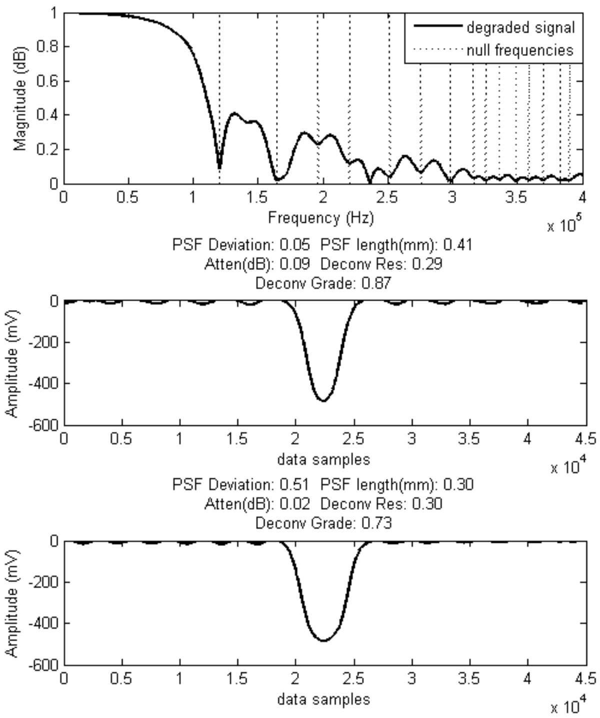

Figure 6. Null frequencies in the spectrum of the degraded pulse. Result of restoration with detected null frequencies, expected PSF length of 0.4mm.

4. Conclusion & Discussion

Algorithm showed superior performance while a rough prior knowledge of L_h was provided for the fuzzy inference system, and the $\Delta E_i = (|E_1 - E_2|)$ had been greater than 0.5, therefore, clearly identifying and segregating the correct deconvolution process. The algorithm was also tested without including the PSF knowledge, in which case ΔE_i was in the interval of 0.1 to 0.5, which was enough to confidently separate the correct deconvolution process.

Figure 6 depicted a special case where H had a null frequency at ω_h = 120 kHz with a normalized magnitude of 0.09, whereas, F null was at ω_f = 170 kHz with a magnitude of 0.02, and had 4 times higher attenuation. Although, ω_f had a magnitude that was in its favor, whereas, the PSF deviation of 0.51 was not. The PSF deviation had outwaited its low magnitude and the correct restoration was successfully distinguished with 14% separation in the deconvolution grades ($|E_1 - E_2|$= 0.14). This high attenuation of ω_f was most likely due to it being closer to the second harmonic of ω_h and, therefore, experienced further attenuation. Nevertheless, owing to the FIS implementation, the correct restoration process had been identified. All the possible rules were considered for the implementation of this FIS and its tuning was performed heuristically by an expert. However, clustering algorithms could be used for FIS with multiple inputs and membership functions to determine the optimum number of rules. Furthermore, adaptive FISs can be used to automate the tuning and learning process of the FIS in a more complicated and complex scenario.

Acknowledgments: Author would like to A. Faghihi for his help and cooperation, also V. Jefimovs for his laboratory assistance. Many thanks to NSIRC, TWI Ltd and for providing the measurement facilities.

Conflicts of Interest: The authors declare no conflict of interest.

References

1. H.-J. Zimmermann, "Fuzzy control," in *Fuzzy Set Theory—and Its Applications*, Springer, 1996, pp. 203-240.
2. A P. Jansson, L. da silva, P. B. Crilly, A. Bernardi. Improving the convergence rate of johnson's deconvolution method. *Instrumentation and Measurement, IEEE Transaction on,* Vol. 51, pp. 1142-1144, 2002.
3. S. M. Riad, A. Bennia. An optimization technique for iterative frequency domain deconvolution. *Instrumentation and measurement, IEEE Transaction on*, vol. 39, pp. 358-362, 1990.

4. S. M. Riad, P. Bidyut. Study and performance evaluation of two iterative frequency-domain deconvolution techniques. *Instrumentation and Measurement, IEEE Transaction on,* vol. 33, pp. 281-287, 1984.
5. B. Parruck and S. M. Riad, "Study and performance evaluation of two iterative frequency-domain deconvolution techniques," *IEEE transactions on instrumentation and measurement,* vol. 33, pp. 281-287, 1984.
6. S. Hosseinzadeh, "Unsupervised spatial-resolution enhancement of electron beam measurement using deconvolution," *Vacuum,* vol. 123, pp. 179-186, 2016.
7. S. Tiwari, V. P. Shukla, A. K. Singh and S. R. Biradar, "Review of motion blur estimation techniques," *Journal of Image and Graphics,* vol. 1, pp. 176-184, 2013.
8. A. Bennia and S. M. Riad, "An optimization technique for iterative frequency-domain deconvolution," *IEEE transactions on instrumentation and measurement,* vol. 39, pp. 358-362, 1990.
9. W. Y. Lo and S. M. Puchalski, "Digital image processing," *Veterinary Radiology & Ultrasound,* vol. 49, pp. S42--S47, 2008.
10. M. E. Moghaddam and M. Jamzad, "Linear motion blur parameter estimation in noisy images using fuzzy sets and power spectrum," *EURASIP Journal on Advances in Signal Processing,* vol. 2007, p. 068985, 2006
11. S. Hosseinzadeh, "Electron Beam Measurement Using Deblurring (deconvolution)," 2016. [Online]. Available: https://uk.mathworks.com/matlabcentral/fileexchange/60414-electron-beam-measurement-using-deblurring-deconvolution.
12. A. Ferrero, A. Federici and S. Salicone, "Instrumental uncertainty and model uncertainty unified in a modified fuzzy inference system," *IEEE Transactions on Instrumentation and Measurement,* vol. 59, pp. 1149-1157, 2010.
13. A. Bennia and S. M. Riad, "Filtering capabilities and convergence of the Van-Cittert deconvolution technique," *IEEE Transactions on Instrumentation and Measurement,* vol. 41, pp. 246-250, 1992.
14. J. Zhao and B. K. Bose, "Evaluation of membership functions for fuzzy logic controlled induction motor drive," in *IECON-PROCEEDINGS-*, 2002.
15. L. A. Zadeh, "Toward a theory of fuzzy information granulation and its centrality in human reasoning and fuzzy logic," *Fuzzy sets and systems,* vol. 90, pp. 111-127, 1997.